Dynamics of Solar and Stellar Convection Zones and Atmospheres
Proceedings IAU Symposium No. 365, 2024
A. V. Getling & L. L. Kitchatinov, eds.
doi:10.1017/S174392132300546X

Rotational shear in the low photosphere of the Sun

T. Corbard, M. Faurobert, B. Gelly, R. Douet and D. Laforgue

University Cote d'Azur, Cote d'Azur Observatory, CNRS UMR7293 J.L. Lagrange laboratory CNRS-IRL2009
email: thierry.corbard@oca.eu

Abstract. We present a new method to measure the rotational height gradient in the solar photosphere. The method is inspired from differential interferometric techniques, we applied it to spectroscopic observations in the FeI 630.15 nm obtained at the solar telescope THEMIS which is equipped with an efficient adaptive optics system. The spectroscopic data was used to obtain images of the granulation at different line cords formed at different heights in the photosphere. Cross-correlation allows us to measure small systematic shifts between similar images. When observations are performed out of the center of the solar disk, the perspective effect gives rise to a radial shift between images formed at different heights. The measurement of this shift provides us with their formation-height difference. At the center of the disk the perspective effect vanishes but we measured a systematic retrograde shift along the east/west direction of the images formed at higher heights. The measured shifts are proportional to the formation height of the images. We interpret these findings as the evidence of a decrease of the rotational velocity with height in the low photosphere of the Sun and we give an estimate of this gradient.

Keywords. Sun: photosphere, differential rotation, High angular resolution

1. Introduction

Rotational shear plays a major role in driving the stellar dynamo. In the Sun, helioseismic observations allow to probe the rotational profile in the convection zone. They have revealed two regions that show a strong height-gradient of the rotation rate, namely, the tachocline at the base of the the convective zone and the near surface shear layer (NSSL). By using observations of surface gravity modes (f-modes), observed by the Michelson Doppler Imager (MDI) onboard the Heliospheric Observatory (SoHO), Corbard and Thompson (2002) were able to obtained a clean measurement of the mean radial gradient of the angular velocity in the sub-surface layer, from about 4 Mm below the surface down to 9 Mm. Ring-diagram analysis by Zaatri and Corbard (2009) using Global Oscillation Network Group data over 7 years also showed that the amplitude of the radial gradient increases closer to the surface in layers above 5 Mm. More recent global and local helioseismology results (Reiter et al. 2020; Komm 2022) covering longer periods and a full solar cycle have confirmed that the gradient of rotation is not uniform in the NSSL and that the rotation rate exhibits a steep decrease close to the surface.

On the theoretical side, in a recent paper devoted to radiative hydrodynamic numerical simulations of the near-surface of the sun in the presence of rotation, Kitiashvili et al. (2023) derived a strong negative gradient in the angular velocity in a subsurface layer at depths smaller than 4 Mm.

In the present work, we are interested in the rotation profile in the photospheric layer. Depth variations in the rotational velocity have been investigated in Livingston and Milkey (1972) by measuring the Doppler effect in several photospheric lines. This did not show any evidence of a rotational depth gradient. However, using a new analysis of 5 mn solar p-mode limb oscillations from 3.5 years of the Helioseismic and Magnetic Imager (HMI) data, Cunnyngham et al. (2017) measured a steep radial decrease of the latitudinal average of the solar rotation rate in the upper photosphere.

In this work, we report the detection of a steep rotational shear at the equator in the low photosphere. The detection does not rely on the Doppler effect but on the measurement of systematic shifts between simultaneous images of the granulation taken at different altitudes. In the field of view (along the spectrograph slit and at many slit positions), we have observed a large number of granular structures. To extract statistical information on possible systematic effects we performed ensemble averages of the Fourier cross-spectra among simultaneous images at different levels in the FeI 630.15 nm line. If the images are similar but slightly shifted the phase of the cross-spectrum shows a linear behavior with respect to the spatial frequency, the slope of this linear trend is directly related to the image shift. Systematic shifts may arise from two different effects, namely, a perspective effect in the radial direction when the images are taken away from the center of the solar disk or horizontal shifts that are induced by a height-gradient of large scale horizontal velocities projected on the plane of the sky. Other kinds of turbulent motions would not lead to any measurable systematic shift. The horizontal shift of a structure is proportional to the duration of the dragging of the upper layer by the velocity gradient namely here, to the correlation time of the granulation pattern (see the sketch in Fig. 1). On average the shift Δx measured at the center of the disk along the equator is given by $\Delta x = \Delta v_{rot}(z)\tau$, where $\Delta v_{rot}(z)$ is the difference in the rotation velocity at the altitude z and τ is the coherence time of the granulation pattern. We used the perspective effect to measure the formation height of the images at different line-cords and an independent measurement of the correlation time by Title et al. (1988) to derive an estimate of the rotational-velocity height gradient. In the next Section we describe our observations and method, in the third Section we present the results, the last Section is devoted to some concluding remarks.

2. Observations and methods

We used spectroscopic observations obtained at the solar telescope THEMIS dating from July, 18 to July 22, 2022, in the FeI 630.15 nm line. We also used HINODE Solar Optical Telescope (SOT) spectropolarimetric (SP) data from the irradiance program, HOP79, performed on July 21, 2022. With THEMIS, we scanned 40"x 108" quiet solar regions at different positions along the west-east central axis and along the south-north polar axis. The HOP79 irradiance program performs montly systematic scans of 30"x130" regions at 20 positions along the polar axis. The pixel size along the slit is 0.235" at THEMIS and 0.32" on SOT-SP, the spectral pixel is 1.35 pm at Themis and 2.1 pm on SOT-SP. A clear advantage of HINODE is the absence of seeing-induced image degradation. With THEMIS, we were able to benefit from some good weather conditions and of the Adaptative Optic system (AO) (Thiébaut et al. 2022; Gelly et al. 2016). We further selected the best spectrograms with a quality criteria based on the root mean square (rms) contrast of the granulation in the continuum along the slit.

To measure a very small displacement between images in the continuum and in the line-wings, we used the phase of their cross-spectrum. This method requires us to consider the power spectra of intensity fluctuations in images taken rigorously at the same time in the continuum and in the line. Actually, 2D images are not needed as far as the spectrograph slit is oriented in the direction of the displacement. In practice, we used

https://doi.org/10.1017/S174392132300546X Published online by Cambridge University Press

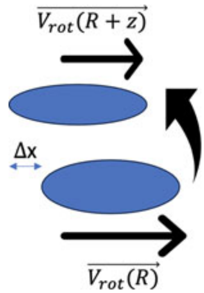

Figure 1. Sketch of the bending of granular structures in the equatorward direction due to a rotational shear.

1D power spectra of the intensity variations along the spectrograph slit and we summed over all the slit positions. Using $I_i(x)$ and $I_c(x)$ to denote the 1D cuts of the line-wing and continuum images, respectively, and assuming that the line-wing image is similar to the continuum one, but slightly displaced at a distance δ, we write $I_i(x) \sim I_c(x-\delta)$ and subsequently, $\widehat{I}_i(u) \sim \widehat{I}_c(u)\exp(2i\pi\delta u)$.

We used a series of spectrograms to estimate the cross-spectrum $\widehat{Q}_{ci}$ between $I_c(x)$ and $I_i(x)$ defined as

$$\widehat{Q}_{ci}(u) =< \widehat{I}_c(u)\widehat{I}_i^*(u) >, \tag{1}$$

where $\widehat{I}_i^*(u)$ represents the conjugate Fourier transform of $I_i(x)$ and the brackets refer to the ensemble average. For similar but shifted images we thus get

$$\widehat{Q}_{ci}(u) \sim <\mid \widehat{I}_c(u) \mid^2> e^{-2i\pi\delta u}. \tag{2}$$

A linear fit of the phase variation with respect to the spatial frequency variable u allows us to measure δ. We note that a positive shift corresponds to a negative slope of the phase. We stress here that this method is not limited by the spatial resolution of the instrument. The main limitation is the signal-to-noise ratio (S/N) of the image spectrum and on the validity of the assumption of similarity between the line-wing and continuum images.

To apply this technics we first construct images formed on surfaces at roughly constant continuum optical depth. Our reconstruction method relies on the relation between the line and continuum absorption coefficients in the Lorentzian damping wings of a line. This is presented in detail in Faurobert et al. (2012) where the method is tested in the framework of the Milne–Eddington approach and applied to Hinode observations. Figure 2 shows a vertical cut of the granulation along the spectrograph slit obtained from 25 line cords in the FeI 630.15 nm line observed with SOT/SP onboard HINODE. The altitudes at disk center of the line-core formation depth and of the contrast inversion layer are derived in Faurobert et al. (2012) and in Faurobert et al. (2013), respectively.

3. Results

Figure 3 illustrates the measurement of the formation height of the line-cord images from the perspective effect. It shows the phase of the cross-spectrum of the images at line cords 16 and 25 (continuum) obtained along the north/south polar axis at an heliocentric angle of 42° in the southern and northern hemispheres both with THEMIS and HINODE data. We do observe a linear behavior of the phase at spatial frequencies smaller than 0.6 arcsecond^{-1}, at larger frequencies it becomes noisy due to a lower signal-to-noise ratio

https://doi.org/10.1017/S174392132300546X Published online by Cambridge University Press

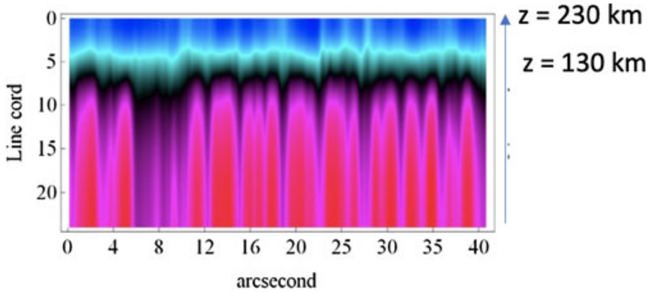

Figure 2. A vertical cut of the solar granulation along the spectrograph slit at the center of the solar disk obtained from SOT/SP data by using 25 line cords in the FeI 630.15 nm. The spectrograph slit is along the North-South axis. The contrast-inversion layer appears in black.

of the reconstructed images at small scales. We observe that the phase shows opposite values in the two hemispheres, in agreement with the perspective effect. A linear fit in the interval [-0.6, 0.6] yields $z = 21.6$ km $\pm$ 0.9 km for the image formation height above the continuum level.

Figure 4 shows, as an example, the cross-spectrum phase derived at the center of the disk between the images in the continuum and at line cord 15, with the spectrograph slit along the north/south and east/west directions. In the last case we show the results obtained for three different observing days. No shift of the images is observed along the polar axis (the phase is noisy but remains close to 0), whereas we do observe a linear behavior of the cross-spectrum phase when the slit is along the equator. This allows us to measure the shift Δx, that it is negative meaning that the rotational velocity decreases with height. For the line cord shown here we get $\Delta x = -22.3 \pm 1.3$ km. In Faurobert et al. (2023) it is shown, using several line cords that Δx is proportional to the height z (obtained from the perspective effect) in the low photosphere with $\Delta x \sim -0.79\,z$. The measurements are made on a very thin layer within 30 km above the continuum level. We interpret these observations as the signature of a negative height gradient of the angular velocity of the following form: $\Omega(R+z) = \Omega(R)(1-\alpha z)$.

Estimating the value of α requires the knowledge of the coherence time of the granulation pattern. Its value was measured by Title et al. (1988) who found that $\tau = 440$ s. Then using the value of the rotational velocity at the continuum level $v_{rot}(R) = 2$ km/s, we obtain $\alpha \simeq 9.\,10^{-4}$ km^{-1}. This leads to a decrease of the angular velocity $\Delta\Omega$ of about -23μrd/s at $z = 100$ km.

4. Concluding remarks

The rotational shear we obtain here is steeper by a factor of 4 than the result found by Cunnyngham et al. (2017). We do expect to find a steeper gradient because they measured a latitudinal average of the angular velocity over some effective heights whereas we measure the rotational shear at the center of the disk close to the equator, and we have more precise values for the altitudes of the measurements. Nevertheless we want to stress that our result depends of the coherence time of the structures that give rise to the signal. We remark that the linear behavior of the cross-spectrum phase is observed at spatial scale smaller than 0.6 arcsecond^{-1}, i. e. at scales larger than 1.6 arcseconds. So it seems that the signal comes mainly from the largest granules that have longer lifetimes. Increasing the value of τ would decrease our estimate of the rotational shear. This issue has to be addressed in future works.

https://doi.org/10.1017/S174392132300546X Published online by Cambridge University Press

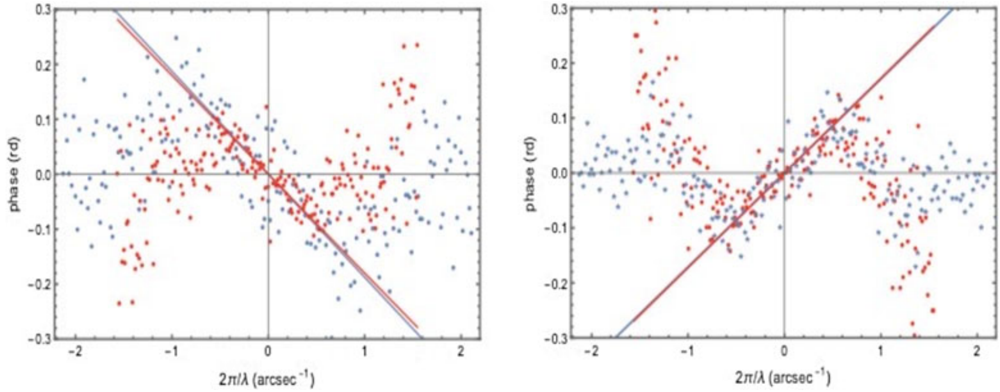

Figure 3. Phase of the cross-spectrum of images at cords 16 and 25 (continuum) with the slit along the north/south axis at two symmetrical position on the polar axis. Blue symbols: from Themis data, red symbols: from Hinode data. **Left:** In the southern hemisphere, **Right:** in the northern hemisphere. The straight lines show linear fits at spatial frequencies smaller than 0.6 arcsec^{-1}.

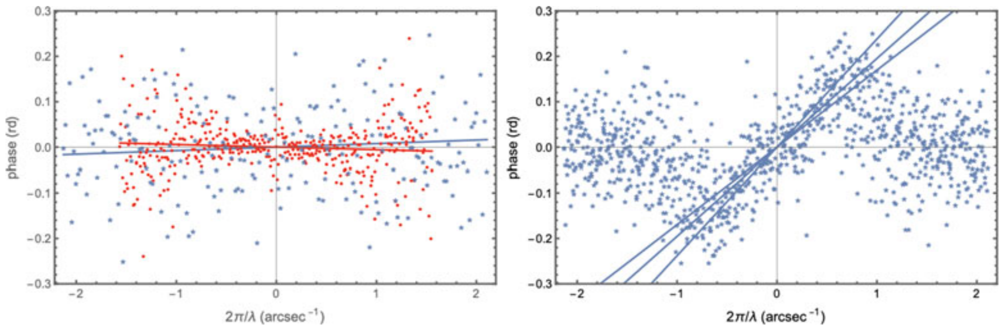

Figure 4. **Left:** Phase of the cross-spectrum of images at cords 15 and 25 (continuum) with the slit along the polar axis. Blue symbols: from Themis data, red symbols: from Hinode data. **Right:** Phase of the cross-spectrum with the slit along the equator for three different observing days. The straight lines show linear fits at spatial frequencies smaller than 0.6 arcsec^{-1}.

We also remark that a height decrease of the rotational velocity could be misinterpreted as a latitudinal decrease because measurements at high latitudes are performed at smaller limb-distances i.e. at higher altitudes than measurements at low latitudes.

References

Corbard, T. & Thompson, M. J. 2002, *Solar Phys.*, 205(2), 211–229.

Cunnyngham, I., Emilio, M., Kuhn, J., Scholl, I., & Bush, R. 2017, *Phys. Rev. Lett.*, 118, 051102.

Faurobert, M., Ricort, G., & Aime, C. 2012, *A& A*, 548, A80.

Faurobert, M., Ricort, G., & Aime, C. 2013, *A& A*, 554, A116.

Faurobert, M., Corbard, T., Gelly, B., Douet, R., & Laforgue, D. 2023, *A& A*, 676, L4.

Gelly, B., Langlois, M., Moretto, G., Douet, R., Lopez Ariste, A., Tallon, M., Thiébaut, E., Geyskens, N., Lorgeoux, G., Léger, J., & Le Men, C. In Hall, H. J., Gilmozzi, R., & Marshall, H. K., editors, *Ground-based and Airborne Telescopes VI* 2016,, volume 9906 of *Society of Photo-Optical Instrumentation Engineers (SPIE) Conference Series*, 99065A.

Kitiashvili, I. N., Kosovichev, A. G., Wray, A. A., Sadykov, V. M., & Guerrero, G. 2023, *MNRAS*, 518(1), 504–512.

Komm, R. 2022, *Frontiers in Astronomy and Space Sciences*, 9, 1017414.

https://doi.org/10.1017/S174392132300546X Published online by Cambridge University Press

Livingston, W., & Milkey, R.1972, *Solar. Phys.* 25, 267

Reiter, J., Rhodes, E. J., J., Kosovichev, A. G., Scherrer, P. H., Larson, T. P., & , S. F. Pinkerton, I. 2020, *ApJ*, 894(1), 80.

Thiébaut, É., Tallon, M., Tallon–Bosc, I., Gelly, B., Douet, R., Langlois, M., & Moretto, G. In Schreiber, L., Schmidt, D., & Vernet, E., editors, *Adaptive Optics Systems VIII* 2022,, volume 12185, 1218507. International Society for Optics and Photonics, SPIE.

Title, A., Tarbell, T., Topka, K., Acton, L., Duncan, D., Ferguson, S., Finch, M., Frank, Z., Kelly, G., Lindgren, R., Morrill, M., Pope, T., Reeves, R., Rehse, R., Shine, R., Simon, G., Harvey, J., Leibacher, J., Livingston, W., November, L., & Zirker, J. 1988, *Astrophysical Letters and Communications*, 27, 141.

Wöhl, H., Kučera, A., Rybák, J., & Hanslmeier, A. 2002, *A& A*, 394, 1077–1091.

Zaatri, A. & Corbard, T. In Dikpati, M., Arentoft, T., González Hernández, I., Lindsey, C., & Hill, F., editors, *Solar-Stellar Dynamos as Revealed by Helio- and Asteroseismology: GONG 2008/SOHO 21* 2009,, volume 416 of *Astronomical Society of the Pacific Conference Series*, 99.